Molecular Therapy
Nucleic Acids
Original Article

miR-320a induces pancreatic β cells dysfunction in diabetes by inhibiting MafF

Hengzhi Du,[1,2] Zhongwei Yin,[1,2] Yanru Zhao,[1,2] Huaping Li,[1,2] Beibei Dai,[1,2] Jiahui Fan,[1,2] Mengying He,[1,2] Xiang Nie,[1,2] Cong-Yi Wang,[3] Dao Wen Wang,[1,2] and Chen Chen[1,2]

[1]Division of Cardiology, Department of Internal Medicine, Tongji Hospital, Tongji Medical College, Huazhong University of Science and Technology, 1095# Jiefang Ave., Wuhan 430030, China; [2]Hubei Key Laboratory of Genetics and Molecular Mechanisms of Cardiological Disorders, Wuhan 430030, China; [3]The Center for Biomedical Research, Department of Respiratory and Critical Care Medicine, NHC Key Laboratory of Respiratory Diseases, Tongji Hospital, Tongji Medical College, Huazhong University of Sciences and Technology, 1095 Jiefang Ave., Wuhan 430030, China

A variety of studies indicate that microRNAs (miRNAs) are involved in diabetes. However, the direct role of miR-320a in the pathophysiology of pancreatic β cells under diabetes mellitus remains unclear. In the current study, islet transplantation and hyperglycemic clamp assays were performed in miR-320a transgenic mice to explore the effects of miR-320a on pancreatic β cells *in vivo*. Meanwhile, β cell-specific overexpression or inhibition of miR-320a was delivered by adeno-associated virus (AAV8). *In vitro*, overexpression or downregulation of miR-320a was introduced in cultured rat islet tumor cells (INS1). RNA immunoprecipitation sequencing (RIP-Seq), luciferase reporter assay, and western blotting were performed to identify the target genes. Results showed that miR-320a was increased in the pancreatic β cells from high-fat-diet (HFD)-treated mice. Overexpression of miR-320a could not only deteriorate the HFD-induced pancreatic islet dysfunction, but also initiate pancreatic islet dysfunction spontaneously *in vivo*. Meanwhile, miR-320a increased the ROS level, inhibited proliferation, and induced apoptosis of cultured β cells *in vitro*. Finally, we identified that MafF was the target of miR-320a that responsible for the dysfunction of pancreatic β cells. Our data suggested that miR-320a could damage the pancreatic β cells directly and might be a potential therapeutic target of diabetes.

INTRODUCTION

Diabetes mellitus is a growing public health concern globally and the prevalence of diabetes is predicted to be over 400 million people worldwide.[1,2] The ability of pancreatic β cells to secrete insulin, one of the most critical hormones in the development of diabetes that regulates the utilization and storage of glucose, is central to the pathophysiology of diabetes.[3,4] While there are multifactorial mechanisms involved in diabetes mellitus, it is well accepted that the core is the pancreatic β cells fail to produce enough insulin to meet the body's demand, and islet transplantation is a safe alternative for diabetes patients.[5] Although multiple evidence supports the notion that stresses, for example oxidative stress, induced β-cell apoptosis is an important factor contributing to β-cell loss and the onset of type 2 diabetes, the underlying molecular mechanisms are still unclear.[6]

MicroRNAs (miRNAs), a class of small conserved non-coding RNAs of 19–25 nucleotides, play important roles in various biological processes and diseases mainly by inhibiting target mRNA translation or promoting target mRNA degradation.[7–9] Multiple miRNAs were identified to play key roles in diabetes. For example, miR-92a targeted KLF2 to protect pancreatic β-cell function in diabetes mellitus, while overexpression of miR-708 induced β-cell apoptosis.[10,11] Meanwhile, our previous studies also showed that miR-30 could protect against diabetic cardiomyopathy and diabetic nephropathy.[12–14] Moreover, we found that miR-320a, which was markedly elevated in the peripheral blood of coronary artery disease (CAD) patients and diabetic patients, could aggravate diabetic nephropathy via inhibiting MafB.[15] According to miRBase (https://www.mirbase.org), the human stem-loop mir-320 family consists of hsa-mir-320a, hsa-mir-320b, hsa-mir-320c, hsa-mir-320d, and hsa-mir-320e, among which the mature hsa-miR-320a-3p is previously named as hsa-miR-320; while the only member of murine stem-loop mir-320 family is mmu-mir-320, and the mature mmu-miR-320-3p is previously named as mmu-miR-320, which is conserved to hsa-miR-320a-3p. Therefore, miR-320a usually refers to mature hsa-miR-320a-3p and mature mmu-miR-320-3p (Figure S1). Recently, we found that nuclear miR-320a mediated diabetes-induced cardiac dysfunction by activating transcription of fatty acid metabolic genes to cause lipotoxicity in the heart.[16] These data indicated that miR-320a played very important roles in the development of diabetes complications. However, the role of miR-320a in diabetes is still undefined, especiallyin that little is known about the direct effects of miR-320a on pancreatic β cells.

Received 6 December 2020; accepted 19 August 2021;
https://doi.org/10.1016/j.omtn.2021.08.027.

Correspondence: Division of Cardiology, Department of Internal Medicine, Tongji Hospital, Tongji Medical College, Huazhong University of Science & Technology, 1095# Jiefang Ave., Wuhan 430030, China.
E-mail: dwwang@tjh.tjmu.edu.cn
Correspondence: Division of Cardiology, Department of Internal Medicine, Tongji Hospital, Tongji Medical College, Huazhong University of Science & Technology, 1095# Jiefang Ave., Wuhan 430030, China.
E-mail: chenchen@tjh.tjmu.edu.cn

Maf proteins are classified into two subgroups. The large Mafs, including c-Maf, MafA, MafB and Nrl proteins, comprise an acidic transactivation domain in their N terminus.[17] The small Maf family, including MafF, MafG, MafK, is essential and dynamically regulates transcription factors.[18] Maf family contains a basic leucine zipper that mediates dimer formation and targets DNA binding to the Maf recognition element (MARE).[18] Previous studies have shown that small Mafs were required for the activation of stress response factors, anti-oxidant enzymes and proteins involved in the metabolism of xenobiotics.[19] For example, conditional overexpression of MafK in erythroleukemia cells could induce erythroid cell differentiation via regulating the activity of transcription factor NF-E2.[20] More importantly, the role of MafF in β cells is gradually being discovered. As a primary regulator of the anti-oxidant response, transcription factor Nrf2 protected β cells from oxidative stress-induced damage in diabetic mice.[21] And Nrf2-activated anti-oxidant gene expression required its dimerization with small Maf proteins, especially MafF.[19] On the other hand, inhibition of MafF reduced the expression of anti-oxidant genes and increased oxidative stress-induced apoptosis in β cells.[22]

In the present study, we found that overexpression of miR-320a not only deteriorated the HFD-induced pancreatic islet dysfunction, but also spontaneously initiated pancreatic islet dysfunction *in vivo*. Meanwhile, miR-320a suppressed the insulin secretion and induced apoptosis in pancreatic β cells via targeting MafF. These findings suggested that miR-320a was a key regulator in diabetes which could potentially serve as a new therapeutic target.

RESULTS

miR-320a was increased in HFD damaged pancreatic β cells

In order to build a pancreatic β cells injury model, C57BL/6 mice were fed with an HFD for 3, 6, 9 and 12 weeks, respectively. As shown in Figures 1A–C, there were significant increases in body weight, blood glucose, and insulin levels in the HFD group compared with the control group. Moreover, blood glucose changes were statistically significant since the 9th week after high fat feeding, while weight changes were statistically significant at the 12th week compared with the control group. To further test the functional ability of pancreatic β cells to secrete insulin, we performed glucose stimulated insulin release (GSIS) experiments on isolated islets of those mice at each time point. Interestingly, with the prolongation of a high-fat feeding period, insulin release of isolated islets from the HFD group stimulated with glucose was reduced gradually compared with the control group (Figure 1D), which indicated that HFD could damage the function of pancreatic β cells. Using fluorescence *in situ* hybridization (FISH) and immunofluorescence, we found the expression of miR-320a was increased with the prolongation of high-fat feeding period in the cytoplasm of β cells from wild-type (WT) mice pancreatic islets (Figures 1E and S2). Similar results were observed by real-time polymerase chain reaction (PCR) detection (Figure 1F). Meanwhile, the expression levels of other members of the miR-320 family, such as miR-320b, miR-320c, miR-320d, and miR-320e, were not changed by HFD treatment (Figures S3A–S3D). These data indicated that miR-320a might be involved in the HFD-induced damages in pancreatic β cells. To further validate this, we exposed the rat β cell line, INS1, to palmitic acid for 0, 6, 12, 18 and 24 h, respectively. Not only the apoptotic rate of INS1 (Figures 1G and 1H), but also the miR-320a levels (Figure 1I) were increased significantly in a time-dependent manner. We also exposed the human pancreatic β cell line, EndoC-βH1, to palmitic acid for 0, 6, 12, 18 and 24 h, and found the miR-320a levels were increased significantly in a time-dependent manner (Figure S4A). Together, these *in vivo* and *in vitro* data suggested that the increased miR-320a might play an important role in HFD damaged pancreatic β cells.

Overexpression of miR-320a aggravated the HFD-induced damages in pancreatic β cells *in vivo*

Then, miR-320a transgenic (TG) mice were constructed to investigate the effects of miR-320a on β cells *in vivo* (Figure S5A). First, the GSIS experiment was performed on isolated islets from miR-320a TG and wild-type (WT) mice, respectively. As shown in Figure 2A, the insulin secreted by isolated islets from miR-320a TG mice was much less than the islets from WT mice when stimulated with 22 mM glucose. Moreover, a series of studies were conducted to explore the potential effects of miR-320a on insulin secretion *in vivo*. Islet transplantation experiments were performed to investigate whether islets-specific overexpression of miR-320 in would affect glucose homeostasis. We transplanted with an appropriate amount of 100 islets originating either from miR-320 TG or WT mice to streptozocin- (STZ) induced diabetic WT mice (Figure 2B). In marked contrast, mice receiving WT islets (WT-WT) showed immediate restoration of blood glucose control, whereas mice receiving miR-320a TG islets (TG-WT) only exhibited an instable trend of improved blood glucose control 4 days after transplantation (Figure 2C). Although mice receiving islet transplantation almost eventually showed similar restoration of blood glucose control in both groups, more glucose fluctuations and worse glucose control were observed in TG-WT mice during the post-transplantation period compared to WT-WT mice (Figure 2C). In line with the undesirable glycemic control, glucose tolerance at 6 weeks after transplantation was also significantly decreased in mice that received the miR-320a TG islets (Figure S6A), which might due to the damaged *in vivo* insulin secretory response of the miR-320a TG islets (Figure S6B). Together, these data suggested that overexpression of miR-320a in islets was harmful to insulin release of β cells.

To further test the functional ability of pancreatic β cells to secrete insulin in WT-W T or TG-WT groups, we performed hyperglycemic clamp experiments. Plasma glucose was elevated to 20-22 mM in two groups during the hyperglycemic clamp (Figure 2D). In TG-WT mice, a lower dose of glucose infusion (GINF) was needed to clamp glucose at stable state (Figure 2E), indicating that the circulating insulin was inadequate to compensate for insulin utilization compared with WT-WT mice. No significant difference was observed in basal insulin or C-peptide levels between the two groups, whereas the clamp insulin and C-peptide levels of TG-WT group were significantly lower compared to the WT-WT group (Figures 2F and 2G). Importantly,

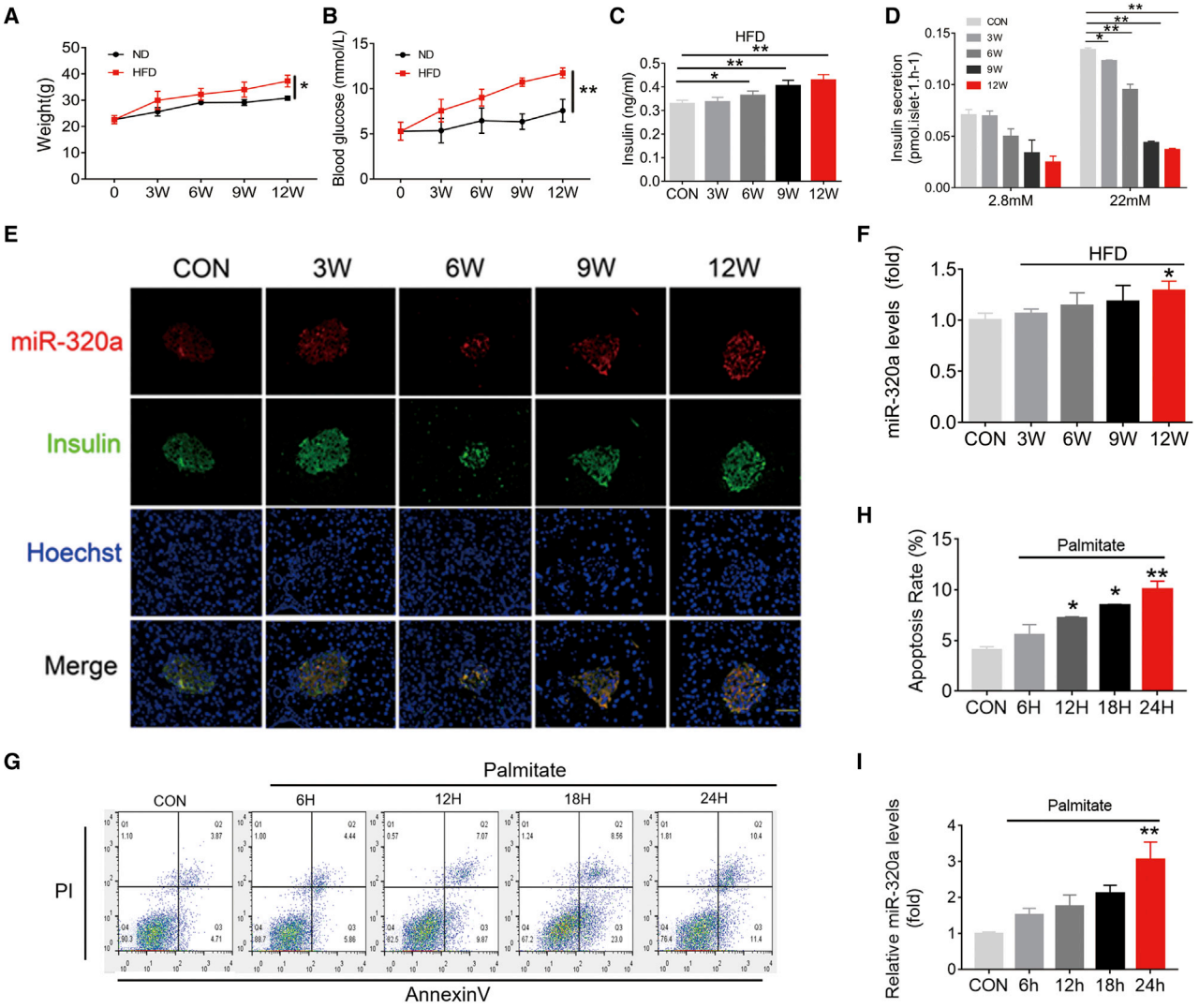

Figure 1. miR-320a was increased in HFD damaged pancreatic β cells

(A) Body weight was measured every three weeks since the age of 8 weeks and results for the 12 weeks; data are expressed as mean ± SEM, n = 6. *p < 0.05, calculated by two-way ANOVA analysis. (B) Blood glucose was measured every three weeks since the age of 8 weeks and results for the 12 weeks; data are expressed as mean ± SEM, n = 6. **p < 0.01, calculated by two-way ANOVA analysis. (C) Insulin level was measured every three weeks since the age of 8 weeks and results for the 12 weeks; data are expressed as mean ± SEM, n = 5. *p < 0.05, **p < 0.01, calculated by one-way ANOVA analysis. (D) Islets were isolated from each time point mice and cultured for 48 h. Then insulin secretion from islets was determined in response to 2.8- or 22-mM glucose; data are expressed as mean ± SEM, n = 3. *p < 0.05, **p < 0.01, calculated by two-way ANOVA analysis. (E) Representative images of immunofluorescence staining for miR-320a (red), insulin (green), and Hoechst (blue) in islets from wild-type mice. Scale bar, 25 μm. (F) Relative miR-320a expression in isolated islets measured by real-time PCR; data are expressed as mean ± SEM, n = 3. *p < 0.05, calculated by one-way ANOVA analysis. (G) and (H) Apoptosis of INS1 were determined by Annexin V/PI flow cytometric analysis; data are expressed as mean ± SEM, n = 3. *p < 0.05, **p < 0.01, calculated by one-way ANOVA analysis. (I) Relative miR-320a expression in INS1 measured by real-time PCR; data are expressed as mean ± SEM, n = 3. *p < 0.05, **p < 0.01, calculated by one-way ANOVA analysis.

decreased function of pancreatic β cell was also highlighted by the inferior insulin disposition index (DIo) in mice receiving miR-320a TG islets (Figure 2H). Moreover, the number of TdT-mediated-dUTP-nick-end-labeling- (TUNEL) positive apoptotic β-cells in the TG-WT mice grafts was significantly increased compared with WT-WT mice (Figure 2I). These data indicated that the increased miR-320a was harmful for insulin release of pancreatic β cells *in vivo*.

Furthermore, we exposed the transplant recipient mice to high-fat feeding, simulating the process of diabetes, to explore the effects of miR-320a on pancreatic β cells during diabetes. The WT-WT and TG-WT mice at 6 weeks post-transplantation, when there was no significant difference in blood glucose between the two groups, were fed with HFD for another 6 weeks. As expected, there were marked increase in blood glucose in both WT-WT and TG-WT mice after

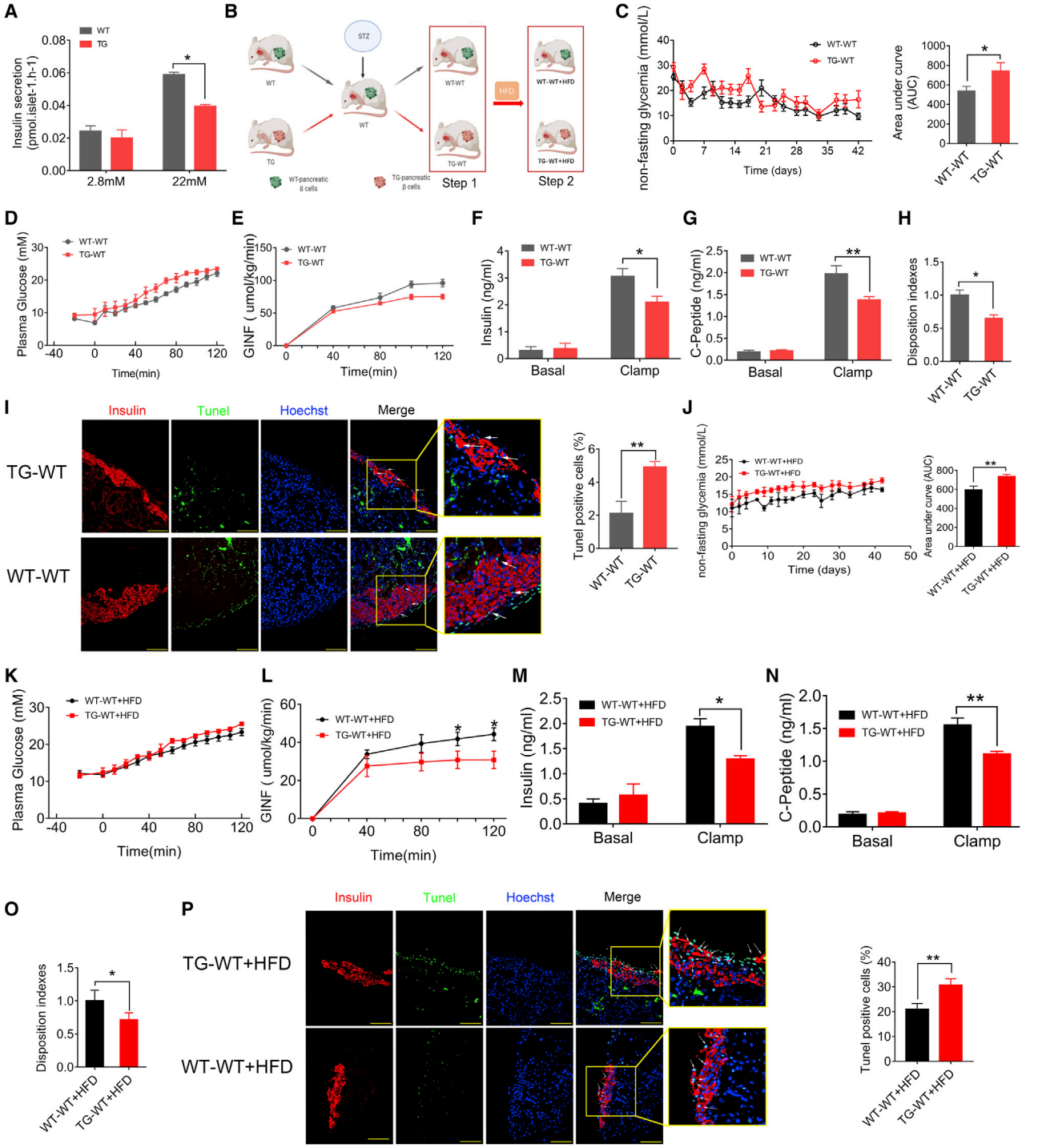

Figure 2. Overexpression of miR-320a aggravated the HFD-induced damages in pancreatic β cells *in vivo*

(A) Pancreatic islets from miR-320a transgenic (TG) or wild-type (WT) mice were isolated and cultured. Insulin secretion was determined in response to 2.8 or 22mM glucose; data are expressed as mean ± SEM, n = 5. *p < 0.05, calculated by two-way ANOVA analysis. (B) Model of islet transplantation. (C) Streptozocin (STZ)-induced diabetic WT mice were transplanted with an appropriate amount (100) of WT islets or miR-320a transgenic (TG) mice islets. Blood glucose levels were monitored for 6 weeks, and results expressed as area under the curve; data are expressed as mean ± SEM, n = 5. *p < 0.05, calculated by Student's t test. Diabetic mice receiving WT or TG mice islets were fasted overnight and glucose tolerance tests (1.0 g/kg body weight) were performed at 6 weeks post-transplant. Diabetic mice receiving WT or TG mice islets were fasted

(legend continued on next page)

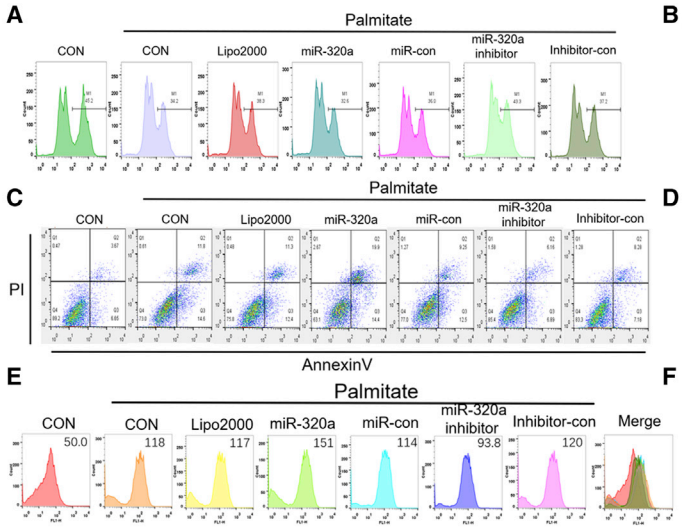

Figure 3. Overexpression of miR-320a damaged pancreatic β cells *in vitro*

INS1 cells were transfected with miR-320a mimics/inhibitors and then subjected to palmitate (0.3 mmol/L) stimulation. (A) and (B) Effects of miR-320a mimics/inhibitors on proliferation were determined by EdU flow cytometric analysis in cultured INS1 cells; data are expressed as mean ± SEM, n = 3. *p < 0.05, calculated by one-way ANOVA analysis. (C) and (D) Effects of miR-320a mimics/inhibitors on apoptosis were determined by Annexin V/PI flow cytometric analysis in cultured INS1 cells; data are expressed as mean ± SEM, n = 3. *p < 0.05, **p < 0.01, calculated by one-way ANOVA analysis. (E) and (F) Effects of miR-320a mimics/inhibitors on the ROS levels were determined by DCFH-DA flow cytometric analysis in cultured INS1 cells; data are expressed as mean ± SEM, n = 3. *p < 0.05, **p < 0.01, calculated by one-way ANOVA analysis.

HFD, and importantly TG-WT mice showed worse control of blood glucose than WT-WT mice (Figure 2J). At 6 weeks post-HFD, glucose tolerance was also significantly decreased in mice that received the miR-320a TG islets (TG-WT+HFD) compared with WT islets recipients (WT-WT+HFD) (Figures S6C and S6D). At the meantime, hyperglycemic clamp experiments were performed. And we found lower GINF, clamp insulin, and C-peptide levels as well as decreased DIo in TG-WT+HFD mice compared with WT-WT+HFD mice, indicating that the insulin secretory capacity of miR-320a TG islets were much worse than WT islets subject to HFD treatment (Figures 2K–2O). Morphologically, we observed significant increase in TUNEL-positive β-cells in the TG-WT+HFD mice grafts compared to WT-WT+HFD mice (Figure 2P).

Of note, these data suggested that overexpression of miR-320a aggravated the damages of HFD in pancreatic β cells, as indicated by worse glucose control, weakened insulin secretion, and increased β cell apoptosis.

Overexpression of miR-320a damaged pancreatic β cells *in vitro*

To further investigate the consequences of miR-320a overexpression in pancreatic β cells, we performed gain/loss-of-function analyses in INS1 cells by transfecting miR-320a mimics/inhibitor. Interestingly, miR-320a mimics inhibited the proliferation (Figures S7A–S7D), induced the apoptosis (Figures S7E and S7F), and increased the ROS level of INS1 cells in comparison with miR-con (Figures S7G and S7H), while miR-320a inhibitor had no effect on INS1 cells under basal conditions. Furthermore, we transfected miR-320a mimics/inhibitor into INS1 cells followed by high-palmitate treatment. Similar to the effects under basal conditions, miR-320a mimics aggravated the decreased proliferation (Figures 3A and 3B), increased apoptosis (Figures 3C and 3D) and ROS level (Figures 3E and 3F) induced by high-palmitate treatment. Moreover, miR-320a inhibitor reversed the effects of high-palmitate on proliferation, apoptosis, and ROS level of INS1 cells compared with inhibitor control (Figures 3A–3F). These data supported that overexpression of miR-320a damaged pancreatic β cells *in vitro*.

miR-320a induced pancreatic β cell dysfunction via targeting MafF

To explore the underlying molecular mechanisms of miR-320a in islet cells, we performed RNA immunoprecipitation sequencing (RIP-seq) using anti-Argonaute2 (Ago2) antibody to identify the potential targets of miR-320a in INS1 cells. Using a cutoff of fold change > 2 and p < 0.05, we identified 86 mRNAs that showed increased association

overnight and hyperglycemic clamp experiments were performed at 6 weeks post-transplant. Plasma glucose (D) and - GINF (E) were measured during hyperglycemic clamps. Insulin (F) and C-peptide levels (G) before and during the last 20 min of the hyperglycemic clamp and (H) disposition indexes (DI = GINF/insulin x C-peptide) during the last 20 min of hyperglycemic clamp in mice; data are expressed as mean ± SEM, n = 5. *p < 0.05, **p < 0.01, calculated by two-way ANOVA analysis. (I) Representative images of immunofluorescence staining for TUNEL (green), insulin (red), and Hoechst (blue) in transplanted islets from WT-WT or TG-WT mice. Scale bar, 10 μm. Data are expressed as mean ± SEM, n = 3, **p < 0.01, calculated by Student's t test. (J) Diabetic mice receiving WT or TG mice islets were fed with high-fat diet for another 6 weeks and blood glucose levels were monitored, and results expressed as area under the curve, data are expressed as mean ± SEM, n = 5. **p < 0.01, calculated by two-way ANOVA analysis. Diabetic mice receiving WT or TG mice islets were fasted overnight and glucose tolerance tests (1.0 g/kg body weight) were performed at 6 weeks post-transplant. Diabetic mice receiving WT or TG mice islets were fasted overnight and hyperglycemic clamp experiments were performed at 6 weeks post-transplant. Plasma glucose (K) and GINF (L) were measured during hyperglycemic clamps. Insulin (M) and C-peptide levels (N) before and during the last 20 min of the hyperglycemic clamp, data are expressed as mean ± SEM, n = 5. *p < 0.05, **p < 0.01, calculated by two-way ANOVA analysis. (O) Disposition indexes during the last 20 min of hyperglycemic clamp in mice; data are expressed as mean ± SEM, n = 5. *p < 0.05, calculated by one-way ANOVA analysis. (P) Representative images of immunofluorescence staining for TUNEL (green), insulin (red), and Hoechst (blue) in transplanted islets from WT-WT+HFD or TG-WT+HFD mice. Scale bar, 10 μm. Data are expressed as mean ± SEM, n = 3, *p < 0.05, calculated by Student's t test.

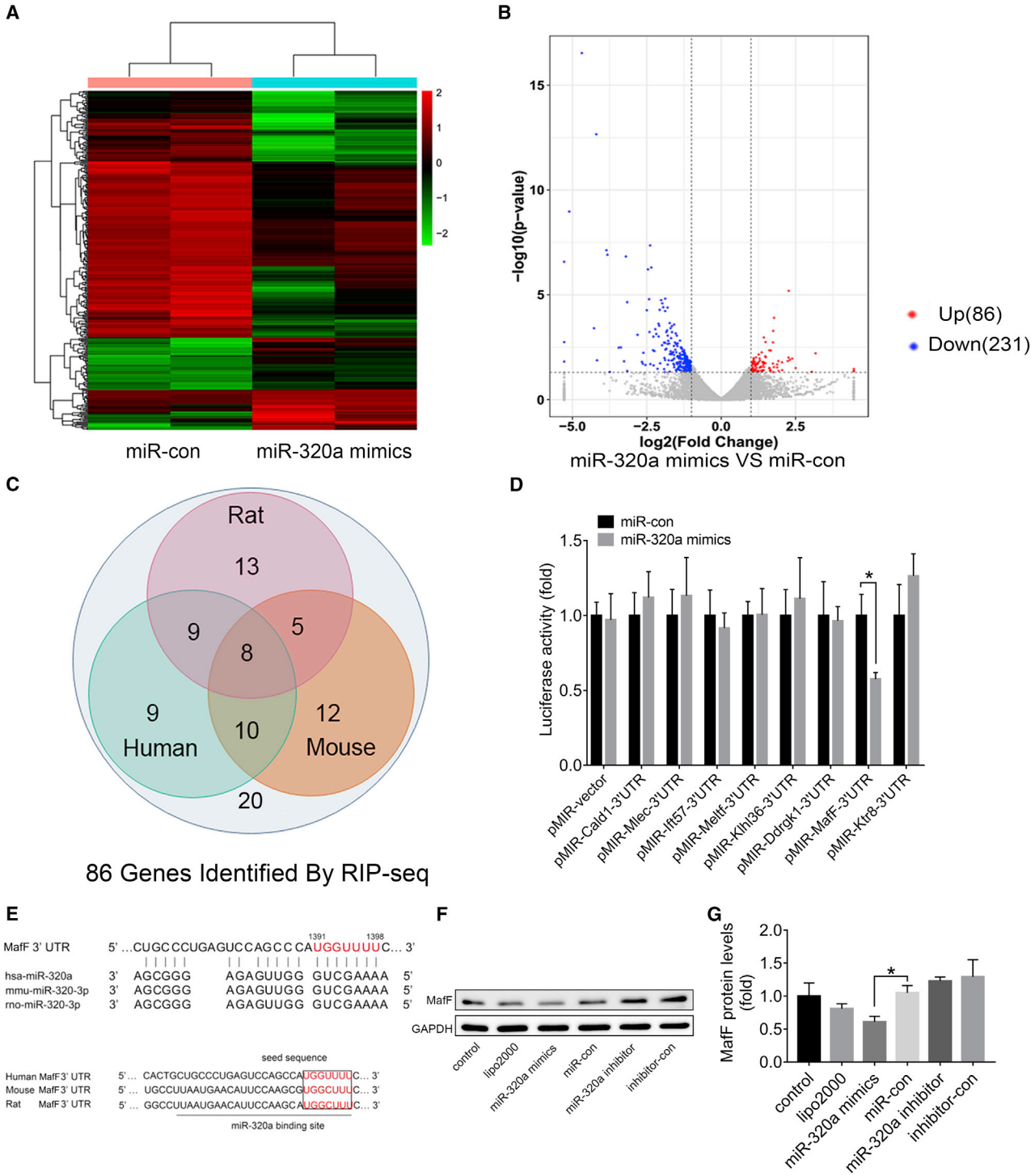

Figure 4. miR-320a suppressed the function of pancreatic β cells via MafF

(A) Heatmap and Volcano plot (B) of the genes in RIP-seq using anti-Ago2 antibody in INS1 cells following miR-320a mimics or miR-con transfection. n = 2. (C) Venn diagram showing the overlap number of candidate target genes of miR-320a identified by Ago2-RIP-seq, which contained the binding sites of miR-320a among rat, mouse, and human species predicted by RNAhybrid. (D) Regulation of miR-320a on 3′-UTR of Ift57, Krt8, Ddrgk1, Cald1, MafF, Mlec, Meltf and Klhl36 in INS1 cells by luciferase reporter assay; data are expressed as mean ± SEM, n = 3. *p < 0.05, calculated by Student's t test. (E) Sequence alignment of binding sites between miR-320a and the 3′-UTR of MafF among several species. (F and G) Relative expression of MafF detected by western blot. Data are expressed as mean ± SEM, n = 3, *p < 0.05, calculated by one-way ANOVA analysis.

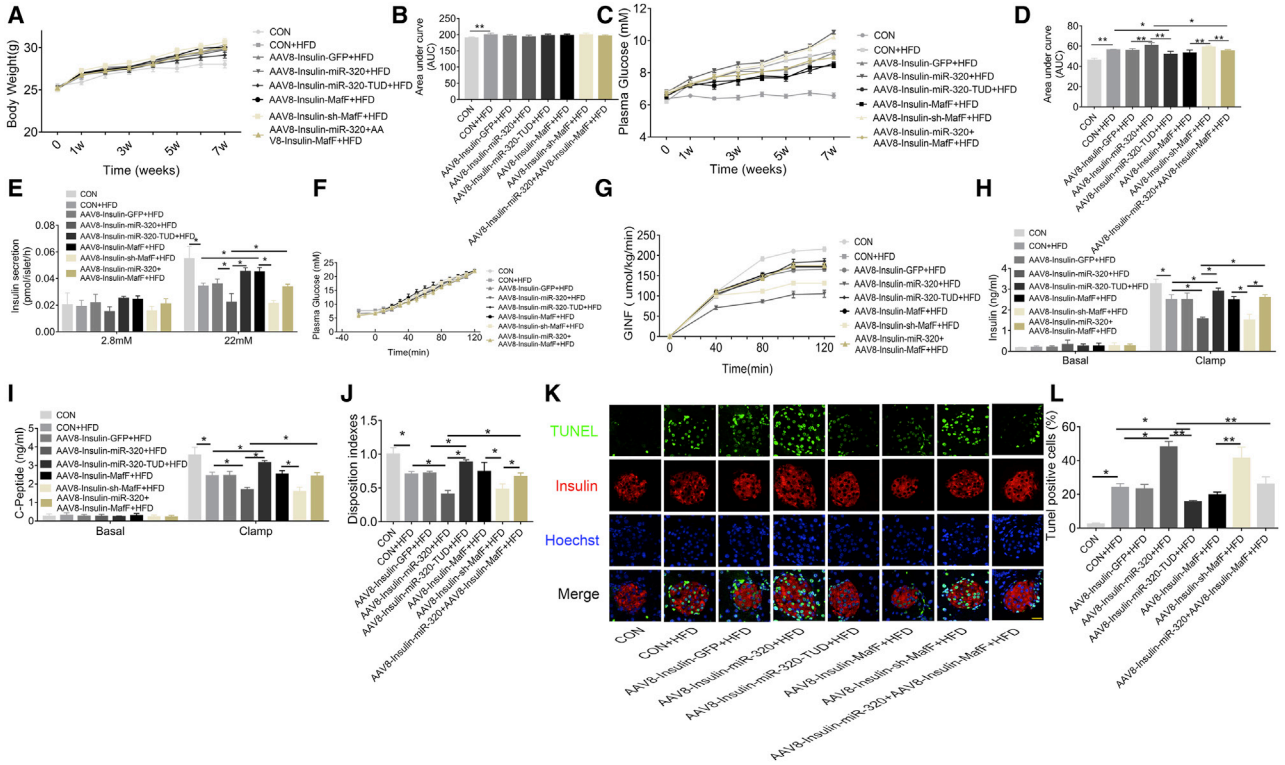

Figure 5. MafF restoration attenuated miR-320a induced pancreatic β cells dysfunction *in vivo*

(A)–(D) Body weight and blood glucose levels were monitored for 7 weeks and results were expressed as area under the curve; data are expressed as mean ± SEM, n = 10. *p < 0.05, **p < 0.01, calculated by one-way ANOVA analysis. (E) Pancreatic islets from mice treated with AAV8-insulin vectors under normal diet were isolated and cultured. Insulin secretion was determined in response to 2.8 or 22mM glucose; data are expressed as mean ± SEM, n = 5. *p < 0.05, calculated by two-way ANOVA analysis. Plasma glucose (F) and GINF (G) were measured during hyperglycemic clamps. (H) and (I) Insulin and C-peptide levels before and during the last 20 min of the hyperglycemic clamp during the last 20 min of hyperglycemic clamp in mice; data are expressed as mean ± SEM, n = 6. *p < 0.05, calculated by two-way ANOVA analysis. (J) Disposition indexes (DI = GINF/insulin x C-peptide) during the last 20 min of hyperglycemic clamp in mice; data are expressed as mean ± SEM, n = 4. *p < 0.05, calculated by two-way ANOVA analysis. (K) and (L) Representative images of immunofluorescence staining for TUNEL (green), insulin (red), and Hoechst (blue) in islets from HFD mice treated with pancreatic β cells specific insulin vectors (AAV8-insulin). Scale bar, 20 μm. Data are expressed as mean ± SEM, n = 5, *p < 0.05, **p < 0.01, calculated by one-way ANOVA analysis.

with the Ago2 protein after miR-320a transfection (Figures 4A and 4B). Then, the online computational tool, RNAhybrid,[23] was used to screen the potential binding sites of miR-320a with these 86 mRNA sequences among rat, mouse, and human species (Table S1). Intersectional analyses of prediction results were shown in the Venn diagram (Figure 4C). The combined overlap resulted in 8 candidate genes, including Ift57, Krt8, Ddrgk1, Cald1, MafF, Mlec, Meltf and Klhl36. Moreover, luciferase reporter assays were performed to identify the effects of miR-320a on specific binding sites in each gene in INS1 cells and HEK293 cells. Among them, only the activity of luciferase reporter containing the 3′ UTR sequence of MafF was obviously suppressed when co-transfected with miR-320a mimics, compared with miR-con (Figure 4D and Figure S8A). Moreover, the binding sites between miR-320a and MafF and were highly conserved among species (Figure 4E). Western blots were performed in INS1 cells for further validation. Among the potential targets, miR-320a mimic transfection only significantly reduced MafF protein level (Figures 4F and 4G, and Figure S9A). These data implied that MafF was a direct target of miR-320a in INS1 cells.

MafF restoration attenuated miR-320a-induced pancreatic β cells dysfunction *in vivo*

To study whether MafF restoration attenuated miR-320a induced pancreatic β cells dysfunction, we employed rAVV8-insulin delivery system in mice under normal or HFD diet (Figures S10A–S10G and S11A–S11G). The body weight of mice in each group were markedly increased after HFD comparing with control group, while no significant change in body weight was observed under normal diet (Figures 5A and 5B and Figures S12A and S12B). Moreover, under both conditions, the worse glucose control and insulin secretory capacity were detected in AAV8-insulin-miR-320 compared with AAV8-insulin-con (Figures 5C–5E and Figures S12C–S12E). Importantly, AAV8-insulin-MafF treatment attenuated the damaged glucose control and insulin secretory capacity in AAV8-insulin-miR-320 mice (Figures 5C–5E and S12C–S12E). It was worth mentioning that the AAV8-insulin-miR-320-TUD alleviated the hyperglycemia and enhanced the insulin secretion compared to AAV8-insulin-con under HFD diet (Figures 5C–5E).

Furthermore, by performing hyperglycemic clamp experiments, we found lower GINF, clamp insulin and C-peptide levels, as well as reduced DIo in AAV8-insulin-miR-320-TUD compared with AAV8-insulin-con under HFD diet, and AAV8-insulin-MafF treatment alleviated the lower GINF, clamp insulin, C-peptide levels as well as decreased DIo and higher TUNEL-positive β-cells in AAV8-insulin-miR-320 mice (Figures 5G–5J and Figures S12G–S12L). These results suggested that miR-320a could deteriorate pancreatic islet function via downregulating MafF expression, while inhibition of miR-320 or MafF restoration might protect pancreatic islet function under high-fat conditions. Western blot assays showed that the ratio of p-AKT/Akt in the muscle, the fat, and the liver was decreased in the HFD condition compared with the normal diet, which suggested that HFD would induce insulin resistance in peripheral organs (Figures S13A–S13F). Moreover, there was no difference in the ratio of p-AKT/Akt among the control, AAV8-insulin-miR-320a-, and AAV8-insulin-MafF-treated mice under high fat or normal diet, suggesting that AAV8-insulin-miR-320a and AAV8-insulin-MafF might not affect peripheral organ insulin sensitivity in mice.

miR-320a damaged pancreatic β cells via inhibiting MafF/Nrf2 complex

We further explored the effects of miR-320a/MafF signal on pancreatic β cells functions and the underlying mechanism. The protein levels of MafF were measured in HFD mice and INS1 cells treated with palmitate. We found the protein level of MafF was decreased in a time-dependent manner in HFD mice (Figures 6A and S14A) or palmitate-treated INS1 cells (Figures 6B and S14B), which was in inverse proportion to the miR-320a levels. As shown in Figures 6C and S15A, we found that miR-320a reduced while the expression vector of MafF restored the protein level of MafF. Consistently, miR-320a mimics inhibited proliferation (Figures 6D and S15B), induced apoptosis (Figure 6E), and increased the ROS level of INS1 cells in comparison with miR-con, while MafF restoration attenuated the effects of miR-320a mimics (Figure 6F).

MafF is a known interacting partner of Nrf2, which plays an important role in the regulation of antioxidant gene expression.[19,24,25] To explore whether miR-320a can affect antioxidant gene expression via inhibiting MafF, western blots and real-time PCR were performed. We found that miR-320a inhibited the mRNA levels of NQO1 and HO-1 without influencing the expression of Nrf2, and that the co-transfection of MafF could reverse the miR-320a-induced reduction, which suggested that miR-320a might reduce the expression of antioxidant genes by suppressing MafF (Figures 6G and S15C). Moreover, the mRNA levels of antioxidant genes Nqo1 and HO-1 were also reduced under HFD and palmitate conditions (Figures 6H, 6I, S16A, and S16B). On the other hand, the levels of γ-GCLC, γ-GCLM, and GSTA2—other downstream antioxidant genes of Nrf2—were unaffected by miR-320a but increased after MafF transfection (Figures S16C–S16E). Importantly, this effect was more obvious after the overexpression of miR-320a or the silence of MafF and was alleviated by the suppression of miR-320a or the overexpression of MafF.

Together, these data strongly indicated that overexpression of miR-320a enhanced the oxidative stress of β cells via the inhibiting MafF/Nrf2 signal pathway to inhibit proliferation and induce apoptosis, thus leading to the reduction of insulin release (Figure 6J).

DISCUSSION

In the present study, we used miR-320a TG mice to perform islet transplantation assays and employed hyperglycemic clamps to demonstrate that miR-320a played an important role in β-cell physiology by inhibiting insulin release and inducing apoptosis. In the T2DM, the pancreatic expression of miR-320a was elevated. The overexpression of miR-320a directly led to the reduction of MafF, which contributed to metabolic abnormalities in the islet, including reduced the secretion of insulin, inhibited pancreatic β cells proliferation, and promoted subsequently pancreatic β cells apoptosis. Moreover, excessive fat uptake in turn, induced miR-320a expression, further promoted the progress of diabetes.

As a systemic metabolic disease, diabetes has two main pathogeneses: one is that pancreatic β cells, in part because of an acquired decrease in β-cell mass, cannot secrete enough insulin to meet the metabolic needs of the body; and the other is insulin resistance.[26] Pancreatic β-cell mass is controlled by several mechanisms, including pancreatic β-cell replication, neogenesis, hypertrophy, and survival.[6] The underlying molecular mechanism proposed for pancreatic β-cell mass reduction is an increase in apoptosis not compensated by adequate β-cell regeneration.[27] Furthermore, the most immediate manifestation of β-cell function is the ability to secrete insulin. Accumulating evidence points to a role for oxidative stress in both processes. High concentrations of blood glucose and free fatty acid (FFA) induce reactive oxygen species (ROS) production in pancreatic β cells with potential pathological consequences.[28,29] Oxidative stress has been reported to lower insulin gene expression via reducing the DNA binding activity of PDX-1, which plays a primary role in maintaining normal β-cell function.[30,31] It has also been reported that increased reactive oxygen impact on the function and survival of the β cells through a variety of mechanisms, including changes in enzyme activity, receptor signal transduction, ion channel transport, dysregulated gene expression, and apoptosis.[32,33] Thus, oxidative stress was the crucial pathologic mechanism of β-cell dysfunction in diabetes.

Multiple studies have demonstrated that miRNAs are important regulators of the islet transcriptome, controlling apoptosis, differentiation, and proliferation, as well as regulating unique islet and pancreatic β-cell functions and pathways, such as insulin expression, processing, and secretion.[34] For example, overexpression of miR-34a, miR-146a, miR-199a-5p, or miR-29 increased the apoptosis of MIN6 pancreatic β cells;[35,36] miR-29 and miR-9 reduced glucose-stimulated insulin secretion of pancreatic β cells.[37] Interestingly, miR-320a is ubiquitously expressed throughout the body, and the expression of miR-320a varies in different models of glucose and lipid metabolism disorders.[38] Our previous work suggested that miR-320a mediated diabetes-induced cardiac dysfunction by causing

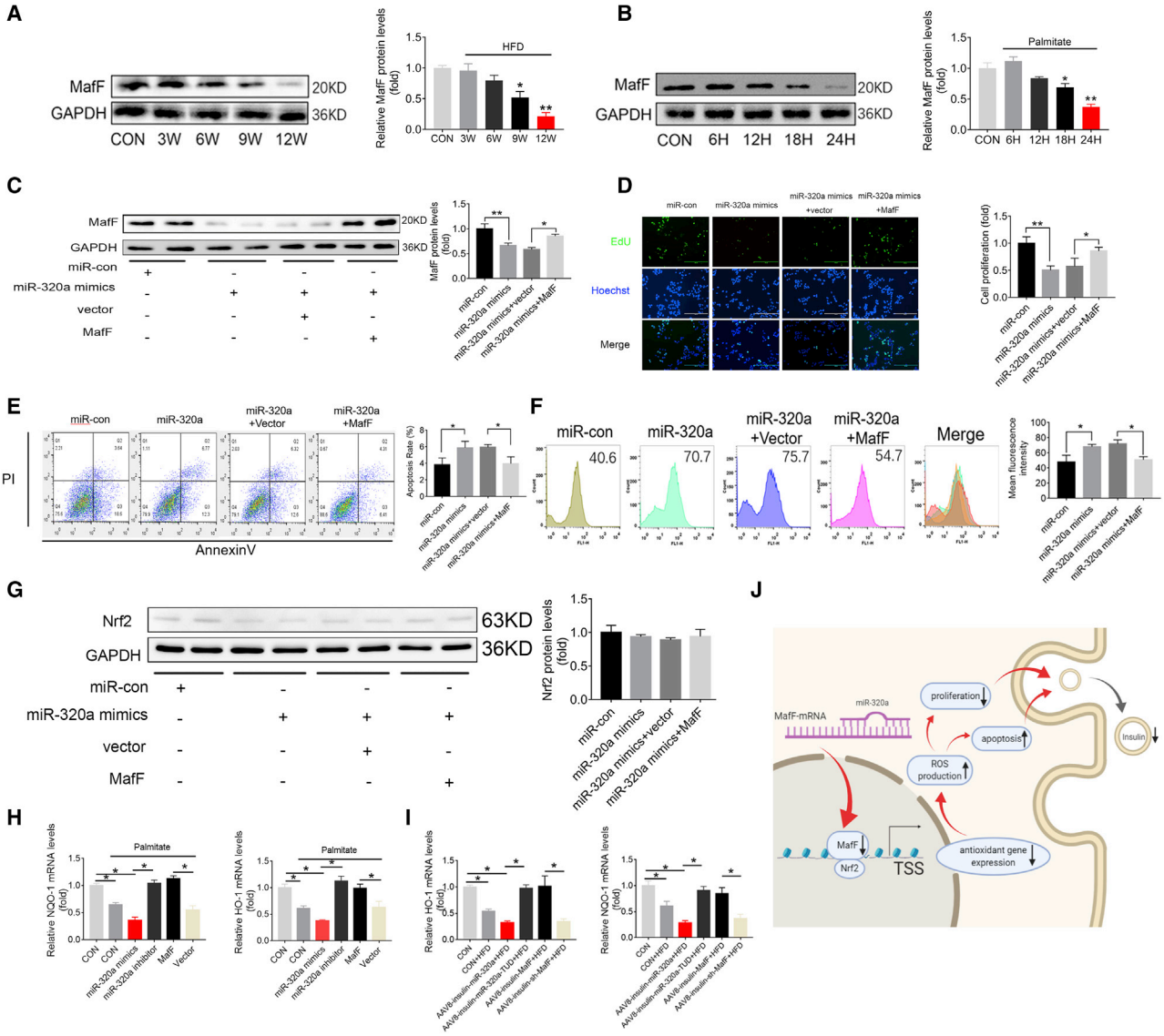

Figure 6. MiR-320a damaged pancreatic β cells via inhibiting MafF/Nrf2 complex

(A) Relative MafF protein levels in HFD mice detected by western blot; data are expressed as mean ± SEM, n = 3. *p < 0.05, **p < 0.01, calculated by one-way ANOVA analysis. (B) Relative MafF protein levels detected INS1 cells treated with palmitate by western blot; data are expressed as mean ± SEM, n = 3. *p < 0.05, **p < 0.01, calculated by one-way ANOVA analysis. (C) Relative MafF protein levels detected by western blot; data are expressed as mean ± SEM, n = 4. *p < 0.05, **p < 0.01, calculated by one-way ANOVA analysis. (D) Proliferation was determined by immunohistochemical staining for EdU (green) and Hoechst (blue) in cultured INS1 cells; data are expressed as mean ± SEM, n = 3. *p < 0.05, **p < 0.01, calculated by one-way ANOVA analysis. (E) Apoptosis was determined by Annexin V/PI flow cytometric analysis in cultured INS1 cells; data are expressed as mean ± SEM, n = 3. *p < 0.05, calculated by one-way ANOVA analysis. (F) The ROS levels were determined by DCFH-DA flow cytometric analysis in cultured INS1 cells; data are expressed as mean ± SEM, n = 3. *p < 0.05, calculated by one-way ANOVA analysis. (G) Relative Nrf2 protein level detected by western blot. (H) Relative mRNA levels of NQO1, HO-1 measured by real-time PCR under HFD conditions; data are expressed as mean ± SEM, n = 3. *p < 0.05, calculated by one-way ANOVA analysis. (I) Relative mRNA levels of NQO1, HO-1 measured by real-time PCR under palmitate conditions; data are expressed as mean ± SEM, n = 3. *p < 0.05, calculated by one-way ANOVA analysis (J) Schematic representation of the role of miR-320a in β cells dysfunction. Overexpression of miR-320a enhanced the oxidative stress of β cells via inhibiting the MafF/Nrf2 signal pathway to increase the ROS level, inhibit the proliferation and induce the apoptosis, thus leading to the reduction of insulin release, which finally impaired the secretion of insulin.

lipotoxicity in the heart,[39] aggravated diet-induced hyperlipidemia, and hepatic steatosis[40] and contributed to renal dysfunction in diabetic nephropathy.[15] Meanwhile, we found that HFD-induced miR-320a was also highly expressed in pancreatic β cells which could directly regulate glucose and lipid metabolism. Therefore, our current research focused on the direct effects of miR-320a on the islet β cells.

We found that the expression of miR-320a was increased in line with the loss of islets functions. Then, hyperglycemic clamp, as the gold standard for evaluating pancreatic β-cell function,[41] was performed to test the mice β-cell function after transplanting miR-320a TG or WT islets into kidney capsules of recipient diabetic mice. It is worth mentioning that $CD4^+$ positive T cells were found in the transplanted islet cells of each group (Figure S17A), but there was no significant difference among groups (Figure S17B), which indicated that the immune response in the transplanted islets was approximately the same in each group and would not affect the original conclusion. Meanwhile, the size of the transplanted islets was relatively subjective. In the current study, islets from miR-320a TG mice were more important for the release of insulin than those WT islets. And overexpression of miR-320a aggravated the damage of HFD to pancreatic β cells, indicating that miR-320a is a key factor in the development of diabetes mellitus. Here, the TUNEL staining showed that the non-islet cell apoptosis seems to also be affected by the AAV8-insulin vectors in both basal and HFD conditions. This may be due to the reduced surrounding islet β-cell function resulting from apoptosis or damage. The pancreatic β cells are the endocrine function region of the pancreas, while the majority of endocrine cells are insulin-secreting β cells.[42] Apart from the function of secreting insulin, β cells can also secrete many pro-angiogenic factors which promote peripheral cell proliferation and influence the function of peripheral cells.[43–46] Thus, the AAV8-insulin-miR-320a-induced paracrine function reduction of islet β cells might also lead to the apoptosis of surrounding cells and functional damage via paracrine effects.

By transfecting miR-320a mimics to become INS1 cells, we found the miR-320a induced the ROS production and apoptosis but inhibited the proliferation of INS1 cells, which were the key factors that affected β-cell mass and function.[6] Moreover, we found it interesting that miR-320a inhibitor had no effect on INS1 cells under basal conditions. This may be due to the low abundance of miR-320a under normal physiological conditions, which was similar to our previous studies in which miR-21 inhibitor showed no effect both *in vitro* and *in vivo*.[47] Notably, INS1 cells were isolated from insulinoma, and miR-320a has been reported to be a tumor suppressor. Although, we have also performed *in vivo* experiments and found that overexpression of miR-320a aggravated the HFD-induced damages in pancreatic β cells from miR-320a TG mice, we could not exclude that miR-320a may cause damage to INS1 cells through other pathways. These data might provide clues to the mechanism that many studies have shown that an increase of miR-320a speeded up the progression of diabetes in patients or animal models with diabetes.[48–50]

It is worth noting that the increase in miR-320a after high-fat feeding was modest but widely expressed *in situ*. This may be because the miR-320a probe could stain not only the mature miR-320a but also the primary miR-320a (pri-miR-320a), and we additionally detected the specificity of the probe in INS1 cells by transfecting miR-320a mimics/inhibitor. Compared with the miR-con group, we could detect that the expression of miR-320a was obviously more, while there was no significant difference between the miR-320a inhibitor and inhibitor group. These results suggested that miR-320a probe is specific (Figure S2B). Meanwhile, the plasma insulin levels appear to increase with increasing time after high-fat feeding. However, insulin secretion seems to be reduced at basal and glucose-stimulated level with time on HFD. This phenomenon is one of the hallmarks of peripheral insulin resistance and is a chronic and cumulative systemic process, which might not represent the ability of pancreatic beta cells to secrete insulin.[51] Under the compensatory condition, the impaired islet beta cells still could be temporarily stimulated to secrete enough insulin to conquer the transient high glucose condition, which is not identical to the condition of systemic hyperinsulinemia or insulin resistance of peripheral organs. Here, we found that miR-320a could further damage the islet beta cells directly but might not affect peripheral organ insulin sensitivity in HFD-treated mice.

In the current study, RIP-seq was performed to identify the mechanism of miR-320a, and we found MafF was the target of miR-320a. MafF is a known interacting partner of Nrf2 that plays an important role in the regulation of antioxidant gene expression such as glutathione S-transferase alpha2 (GSTA2), NAD(P)H:quinone oxidoreductase (NQO1), γ-glutamate cysteine ligase (γ-GCLC and γ-GCLM) and heme oxygenase-1 (HO-1).[19,24,25] In the present study, we found miR-320a inhibited the expression of MafF as well as the antioxidant gene such as NQO1 and HO-1, while Nrf2 was not influenced. It suggested that MafF was the key of miR-320a to induce the oxidative stress and following dysfunction of β cells in diabetes. Interestingly, our lab previous work also showed that another Maf protein, MafB, served as a defender against oxidative stress and apoptosis of podocytes, and was the target genes of miR-320a in diabetic nephropathy.[52]

Diabetes mellitus is a growing public health concern globally. Although multiple evidence supports the notion that stresses, such as oxidative stress, induced β-cell apoptosis is an important factor contributing to β-cell loss and the onset of type 2 diabetes, the underlying molecular mechanisms are still unclear. In our study, we found that the overexpression of miR-320a could induce apoptosis of β cells and aggravate the HFD-induced damages in pancreatic β cells via the blocking MafF signaling pathway, thereby promoting the development of diabetes. Our findings revealed a harmful function of miR-320a in pancreatic β cells. Importantly, we also found that the inhibition of miR-320a could alleviate the HFD-induced damages in pancreatic β cells. Thus, delivery of exogenous miR-320a inhibitor might be a promising treatment strategy for diabetes. These observations provide a theoretical basis for developing miRNA-based therapeutics against diabetes.

MATERIALS AND METHODS

Reagents

RPMI-1640, Dulbecco's Modified Eagle Medium (DMEM), and fetal bovine serum (FBS) were obtained from GIBCO (Grand Island, NY). Lipofectamine 2000 (Lipo2000) reagent was obtained from Invitrogen (Life Technologies Corporation, Carlsbad, CA). The primers for miR-320a and U6 real-time PCR, miR-320a mimics, miR-320a inhibitor, and their controls were purchased from RiboBio (Guangzhou, China).

Antibodies against MafF (Cat No: 12771-1-AP) and CALD1 (Cat No: 66693-1-lg) were procured from Proteintech (Chicago, MA). Antibodies against DDRGK1 (Cat No: bs-8252R) and KLHL36 (Cat No: bs-9628R) were purchased from Bioss (Beijing, China). Antibodies against AKT (Cat No: 4691T) and p-AKT (Cat No: 13038T) were purchased from CST (Cell Signaling Technology, Shanghai, China). Polyvinylidene difluoride (PVDF) membranes were purchased from Millipore (Merck KGaA, Darmstadt, Germany). Horseradish peroxidase-conjugated secondary antibodies and enhanced chemiluminescence reagents were obtained from Pierce Biotechnology (Thermo Fisher Scientific Inc., Rockford, IL). Other reagents were purchased from the Sigma-Aldrich Company, unless otherwise specified.

Cell culture and transfection

Rat islet tumor cells, INS1, were maintained in RPMI-1640 supplemented with 10% FBS and 50 μM β-mercaptoethanol at 37°C with a 95% air, 5% CO_2 atmosphere. Human pancreatic β cell lines, EndoC-βH1 cells (Univercell-Biosolutions, Paris, France), were derived on Matrigel-fibronectin-coated (100 μg/ml and 2 μg/ml, respectively) culture wells. DMEM that containing 5.6 mM glucose, 2% BSA fraction V, 50 uM 2-mercaptoethanol, 10 mM nicotinamide, 5.5 ug/ml transferrin, 6.7 ng/ml selenite, 100 U/ml penicillin, and 100 ug/ml streptomycin was used to maintain EndoC-βH1 cells. For high palmitate stimulation, INS1 cells and EndoC-βH1 cells were treated with palmitate (0.3 mM) for 24 h as described previously.[53] Transfection with miR-320a mimics (100 nM), miRNA inhibitor (100 nM) or relative controls (100 nM) was performed with Lipofectamine 2000 (Invitrogen, Carlsbad, CA), respectively, according to the manufacturer's recommendations.

Animals

The animal study was approved by the Institutional Animal Research Committee of Tongji Medical College. The miR-320a transgenic (TG) mice were kindly generated by Prof. Lianfeng Zhang (Chinese Academy of Medical Sciences, Beijing). Briefly, by performing microinjection according to standard protocols, a DNA fragment containing murine miR-320 was inserted into the pUBC vector for expression under the control of the ubiquitin C promoter to generate miR-320 TG mice. Then, miR-320 TG mice were backcrossed to the background of C57BL/6 for six generations to yield WT and miR-320 TG mice that were >95% of the C57BL/6 genotype. For genotyping miR-320 TG mice, the primers were 5′-CCACTGCTTACTGGC TTATCG-3′ (forward) and 5′-ATGAAGCACCTCCGCTGAG-3′ (reverse). Age- and sex-matched littermates were used as controls. All animals were fed with *ad libitum* access to water and a standard chow diet (6% calories from fat, 21% calories from protein, 71% calories from carbohydrate) or HFD (59% calories from fat, 15% calories from protein, 26% calories from carbohydrate) and housed under a controlled temperature of 22°C and maintained under a 12-hours-light- 12-hours-dark photoperiod. At the end of the experiments, we sacrificed the mice with intraperitoneal injections of a ketamine (80 mg/kg) and xylazine (5 mg/kg) mixture, and tissue samples were snap-frozen in liquid nitrogen or collected for paraffin embedding.[54]

Flow cytometry analyses

INS1 cells were incubated with Annexin V-FITC/PI (BD Biosciences, Sparks, MD) to evaluate cell apoptosis and incubated with DCFH-DA (Beyotime, Nanjing, China) to evaluate intracellular ROS production and incubated with EdU (Meilunbio, Dalian, China) to evaluate cell proliferation.[54,55] After incubation, A FACStar Plus flow cytometer (BD Biosciences, Sparks, MD) was used to analyze the fluorescence signal intensity of cells, as previously described.[56]

Pancreatic islet isolation

Pancreas from 10-week-old to 12-week-old wild-type (WT) and miR-320a TG mice, which were the littermates, were perfused with cold liberase (Cat No:23643124, Roche, IN) solution via the common bile duct, and subsequently islets were removed and incubated at 37°C for 16 min. The Krebs-Ringer Bicarbonate buffer (20 mM HEPES at pH 7.4, 119 mM NaCl, 4.8 mM KCl, 2.5 mM $CaCl_2$, 1.2 mM MgSO4, 1.2 mM KH_2PO4, 5 mM NaHCO3 and 2.8 mM glucose) containing 10% newborn calf serum was used to stop digestion, and then islets were further separated from other pancreatic tissue using a histopque1077 (Sigma-Chemical, Shanghai, China) and hand-picked under a stereomicroscope. Finally, islets were incubated in RPMI-1640 medium (containing 10% fetal calf serum, penicillin and streptomycin, HEPES, 11 mM glucose, and 2 mM glutamine) in a 37°C, 5% CO_2 incubator for 48 h.

Islet transplantation

To establish the diabetes model, 8–10 weeks old recipient C57BL/6 mice were injected with 180 mg/kg streptozotocin (Sigma-Chemical, Shanghai, China) in 10 mM citrate buffer (pH 4.2), then after 2 weeks, mice with blood glucose values $\geq$ 18.8 mmol/l were selected as transplant recipients. Blood glucose levels were determined using a Glucometer (Lifescan, Johnson & Johnson, Shanghai, China). Islets were isolated from pancreas of either miR-320a TG or WT mice, and then transplanted into the streptozotocin-induced diabetes mice as previously describe.[57] In brief, 100 hand-counted islets were transplanted into individual recipient mice. The kidney, for the transplant, was accessed by a left flank incision, and the wound was brought into by gentle blunt dissection. A small nick was made in the kidney capsule at the inferior renal pole, and the miR-320a TG or WT islets were deposited through the nick toward the superior pole of the kidney. The comparable size of islets was hand-picked, and the mass of transplanted β-cell was not significantly different between miR-320a TG and WT mice. Blood glucose levels were then monitored for the next 6 weeks.

Glucose tolerance tests (GTT)

Six-hour-fasted mice were intraperitoneal administered with glucose (1 g/kg body weight), and then GTT were performed. Blood glucose levels were assessed at 0, 15, 30, 60, and 90 min after glucose administration using One-Touch UlteaVue glucometer, respectively (Lifescan, Johnson & Johnson, Shanghai, China). Plasma was collected and stored at −20°C for insulin measurement by using insulin RIA kits (Crystal Chem, Downers Grove, IL).

Glucose-stimulated insulin secretion (GSIS)

Islets were pre-incubated in HEPES-buffered KRB containing 0.1% BSA and 2 mM glucose for 1 h and then experiments were performed in triplicate with batches of five islets incubated at 37°C, 5% CO_2 for 1 h in 100 μL KRB containing 0.1% BSA, supplemented with 22 mM glucose or 2.8 mM glucose. Insulin release was determined by insulin RIA kit (Crystal Chem, Downers Grove, IL).

Hyperglycemic clamp and calculations

The hyperglycemic clamp was performed in 6-hour-fasted conscious mice. Basal insulin and C-peptide were measured at the start of experiments, and then 37.5% glucose was infused to the mice. Blood glucose was maintained at 22 mM by adjusting the rate of glucose infusion through manipulation of frequent, every 10 min, glycemic determination from tail blood. The insulin and C-peptide of sample were taken during the last 20 min of the 120 min hyperglycemic clamp.[58] Blood glucose was measured using a One-Touch UlteaVue glucometer (Lifescan, Johnson & Johnson, Shanghai, China). Sensitivity index (M/I) is calculated according to the following formula: M/I = GINF/insulin; GINF is the rate of glucose infusion, while insulin is the plasma insulin concentration at individual time points during the last 20 min of the hyperglycemic clamp. Disposition index (DI) was calculated according to the following formula: DI = M/I x C-peptide.

Western blots analyses

Bicinchoninic acid assay kit (BOSTER, Wuhan, China) were used to quantify the protein samples from cell and mice pancreas islet. ImageJ program was used to analyze the band intensities of target proteins.

Dual luciferase assay

INS1 cells and HEK293 cells were transfected with 400 ng of pMIR-MafF 3′-UTR, pMIR- CALD1 3′-UTR, pMIR- Ddrgk1 3′-UTR, or pMIR- Klhl36 3′-UTR, respectively. Meanwhile, 100nM miR-320a mimics or control was co-transfected with the reporter plasmids, accompanied with 40 ng of pRL-TK plasmid (Promega, Madison, WI). DualLuciferase Reporter Assay System (Promega, Beijing, China) was used to detect luciferase activity.

Real-time PCR

RNA was isolated from pancreatic islet or INS1 cells with TRIzol reagent (Invitrogen, Carlsbad, CA), and then was reverse-transcribed into cDNA using RevertAid First Strand cDNA Synthesis Kit (Thermo Fisher Scientific, Waltham, MA). Real-time PCR assays were performed using SYBR rapid quantitative PCR Kit (Kapa Biosystems, Woburn, MA)[13]. The relative miRNA levels were determined by normalizing to U6 level using $2^{-\Delta\Delta CT}$ method. Primers were list in Table S2.

RNA immunoprecipitation and RIP-seq

INS1 cells were lysed and then immunoprecipitated with anti-Ago2 antibody (Abnova Corporation, Taiwan, China) or IgG (Abclonal, Wuhan, China) using protein A/G magnetic beads (Thermo Scientific, Shanghai, China) after transfection with miR-320a mimics or miRNA random control for 24 h, as described. The protein A/G magnetic beads were added after incubating the cells overnight at 4°C, and the solution was incubated for 2 h at 4°C. The beads were washed five times with PBS and resuspended in 60 μL Laemmli buffer. The remaining products were extracted with TRIzol, and the levels of mRNA were quantified by real-time PCR. RIP-seq assays were conducted by Personalbio (Shanghai, China).

Immunofluorescent staining and TdT-mediated dUTP nick-end labeling (TUNEL) assay

Formalin-fixed pancreas tissues were paraffin-embedded, cut into 4-mm-thick sections, and stained with anti-insulin antibody (Cat No: A2090, Abclonal, Wuhan, China) or anti-PCAN antibody (Cat No: 2586, Cell Signaling Technology, Shanghai, China) according to the method described previously.[12] TUNEL assay was performed using *in situ* cell death detection kits (Roche Diagnostics GmbH, Mannheim, Germany) to determine the rates of cell apoptosis according to the manufacturer's instructions.[54] For fluorescence *in situ* hybridization (FISH), formalin-fixed paraffin-embedded pancreas sections were hybridized with a miR-320a probe and then incubated with anti-insulin antibody as described previously.[12] Images were acquired by the fluorescence microscopy (Nikon, Tokyo, Japan) and measured by IMAGE PRO-PLUS Software 6.0 (Media Cybernetics, Bethesda, MD).

EdU assays

INS1 cells were exposed to 10 mM 5-ethynyl-2′-deoxyuridine (EdU; (Cat No:C10310-3, RiboBio, China) for 2 h at 37 C° after transfection. Cells were then fixed in 4% PFA for 30 min and permeabilized with 0.5% Triton X-100. Next, the INS1 cells were incubated with the Apollo reaction cocktail (Cat No:C10310-3, RiboBio, China), then stained with Hoechst 33342 for 30 min for DNA content analysis. Finally, the EdU-stained cells were visualized under a fluorescence microscope (Nikon, Tokyo, Japan). The analysis of INS1 cells proliferation was performed using images of randomly selected fields obtained on the fluorescence microscope. The ratio of EDU positive INS1 cells were calculated using the following formula: EDU/Hoechst x 100%, and finally standardized to the control group.

Construction and administration of adeno-associated virus (AAV8)

Male WT mice were divided into various groups (AAV8-insulin-miR-GFP, AAV8-insulin-miR-320, AAV8-insulin-miR-320-TUD, AAV8-insulin-MafF, AAV8-insulin-sh-MafF and AAV8-insulin-miR-320+AAV8-insulin-MafF) under normal feeding condition or high-fat feeding condition, respectively. TUD RNAs containing two single-stranded miRNA-binding sites flanked by double-stranded stems could enhance stability and promote nuclear export as described previously,[59] which is an effective approach that relies on selective sequestration and functional inactivation of the sense strand via codelivered decoy RNAs. For the construction of plasmid expressing MafF, oligonucleotides were designed according to the CDS sequence of MafF (Accession: NM_001130573.1). Then, the oligonucleotides were synthesized and inserted into plasmid by restriction enzyme cleavage.

Statistical analyses

All data, performed using GraphPad Prism Version 7.00 (GraphPad Software, La Jolla, CA), are expressed as mean ± SEM. Student's t tests were used for comparison between the treatment and control groups. The different groups of mice were assessed by two-way ANOVA or repeated-measures ANOVA. The statistical significance of GTT and blood glucose changes were measured by area under curve (AUC) as previously described.[60] Differences were regarded as statistically significant if $^{*}p < 0.05$, $^{**}p < 0.01$.

SUPPLEMENTAL INFORMATION

Supplemental information can be found online at https://doi.org/10.1016/j.omtn.2021.08.027.

ACKNOWLEDGMENTS

We thank our colleagues in Prof. Dao Wen Wang's group for technical assistance and stimulating discussions during the course of this investigation. We thank Prof. Lianfeng Zhang (Institute of Laboratory Animal Science, Peking Union Medical College, Chinese Academy of Medical Sciences, Beijing, China) for the generation of miR-320 transgenic mice. This work was supported by grants from the National Natural Science Foundation of China (nos. 81822002, 31800973, 31771264, 91839302, 81630010, and 81790624) and the Fundamental Research Funds for the Central Universities (2019kfyXMBZ035). The funders had no role in study design, data collection and analysis, manuscript preparation, or decision to publish.

AUTHOR CONTRIBUTIONS

H.D. designed and conducted the experiments and wrote the paper; Z.Y. and Y.Z. designed and conducted the experiments; H.L., B.D., J.F., M.H., X.N., and C.Y.W. participated in designing the experiments; D.W.W. and C.C. designed the experiments and wrote the paper.

DECLARATION OF INTERESTS

The authors declare no conflicts of interest.

REFERENCES

1. Dennis, J.M., Shields, B.M., Henley, W.E., Jones, A.G., and Hattersley, A.T. (2019). Disease progression and treatment response in data-driven subgroups of type 2 diabetes compared with models based on simple clinical features: an analysis using clinical trial data. Lancet Diabetes Endocrinol. *7*, 442–451.
2. Tesfaye, B., Alebel, A., Gebrie, A., Zegeye, A., Tesema Leshargie, C., Ferede, A., Abera, H., and Alam, K. (2019). Diabetes mellitus and its association with hypertension in Ethiopia: A systematic review and meta-analysis. Diabetes Res. Clin. Pract. *156*, 107838.
3. Saltiel, A.R., and Kahn, C.R. (2001). Insulin signalling and the regulation of glucose and lipid metabolism. Nature *414*, 799–806.
4. American Diabetes Association (2014). Diagnosis and classification of diabetes mellitus. Diabetes Care *37* (*Suppl 1*), S81–S90.
5. Vantyghem, M.C., de Koning, E.J.P., Pattou, F., and Rickels, M.R. (2019). Advances in β-cell replacement therapy for the treatment of type 1 diabetes. Lancet *394*, 1274–1285.
6. Rhodes, C.J. (2005). Type 2 diabetes-a matter of beta-cell life and death? Science *307*, 380–384.
7. Bartel, D.P. (2004). MicroRNAs: genomics, biogenesis, mechanism, and function. Cell *116*, 281–297.
8. Rana, T.M. (2007). Illuminating the silence: understanding the structure and function of small RNAs. Nat. Rev. Mol. Cell Biol. *8*, 23–36.
9. Eulalio, A., Huntzinger, E., and Izaurralde, E. (2008). Getting to the root of miRNA-mediated gene silencing. Cell *132*, 9–14.
10. Rodríguez-Comas, J., Moreno-Asso, A., Moreno-Vedia, J., Martín, M., Castaño, C., Marzà-Florensa, A., Bofill-De Ros, X., Mir-Coll, J., Montané, J., Fillat, C., et al. (2017). Stress-Induced MicroRNA-708 Impairs β-Cell Function and Growth. Diabetes *66*, 3029–3040.
11. Wang, W., Wang, J., Yan, M., Jiang, J., and Bian, A. (2018). MiRNA-92a protects pancreatic B-cell function by targeting KLF2 in diabetes mellitus. Biochem. Biophys. Res. Commun. *500*, 577–582.
12. Zhao, Y., Yin, Z., Li, H., Fan, J., Yang, S., Chen, C., and Wang, D.W. (2017). MiR-30c protects diabetic nephropathy by suppressing epithelial-to-mesenchymal transition in db/db mice. Aging Cell *16*, 387–400.
13. Yin, Z., Zhao, Y., He, M., Li, H., Fan, J., Nie, X., Yan, M., Chen, C., and Wang, D.W. (2019). MiR-30c/PGC-1β protects against diabetic cardiomyopathy via PPARα. Cardiovasc. Diabetol. *18*, 7.
14. Fan, J., Li, H., Nie, X., Yin, Z., Zhao, Y., Chen, C., and Wen Wang, D. (2017). MiR-30c-5p ameliorates hepatic steatosis in leptin receptor-deficient (db/db) mice via down-regulating FASN. Oncotarget *8*, 13450–13463.
15. He, M., Wang, J., Yin, Z., Zhao, Y., Hou, H., Fan, J., Li, H., Wen, Z., Tang, J., Wang, Y., et al. (2019). MiR-320a induces diabetic nephropathy via inhibiting MafB. Aging (Albany NY) *11*, 3055–3079.
16. Li, H., Fan, J., Zhao, Y., Zhang, X., Dai, B., Zhan, J., Yin, Z., Nie, X., Fu, X.D., Chen, C., et al. (2019). Nuclear miR-320 mediates diabetes-induced cardiac dysfunction by activating transcription of fatty acid metabolic genes to cause lipotoxicity in the heart. Circ Res. *125*, 1106–1120.
17. Blank, V., and Andrews, N.C. (1997). The Maf transcription factors: regulators of differentiation. Trends Biochem. Sci. *22*, 437–441.
18. Motohashi, H., Shavit, J.A., Igarashi, K., Yamamoto, M., and Engel, J.D. (1997). The world according to Maf. Nucleic Acids Res. *25*, 2953–2959.
19. Katsuoka, F., Motohashi, H., Ishii, T., Aburatani, H., Engel, J.D., and Yamamoto, M. (2005). Genetic evidence that small maf proteins are essential for the activation of antioxidant response element-dependent genes. Mol. Cell. Biol. *25*, 8044–8051.
20. Igarashi, K., Itoh, K., Hayashi, N., Nishizawa, M., and Yamamoto, M. (1995). Conditional expression of the ubiquitous transcription factor MafK induces erythroleukemia cell differentiation. Proc. Natl. Acad. Sci. USA *92*, 7445–7449.
21. Yagishita, Y., Fukutomi, T., Sugawara, A., Kawamura, H., Takahashi, T., Pi, J., Uruno, A., and Yamamoto, M. (2014). Nrf2 protects pancreatic β-cells from oxidative and nitrosative stress in diabetic model mice. Diabetes *63*, 605–618.
22. Bensellam, M., Montgomery, M.K., Luzuriaga, J., Chan, J.Y., and Laybutt, D.R. (2015). Inhibitor of differentiation proteins protect against oxidative stress by regulating the antioxidant-mitochondrial response in mouse beta cells. Diabetologia *58*, 758–770.
23. Rehmsmeier, M., Steffen, P., Hochsmann, M., and Giegerich, R. (2004). Fast and effective prediction of microRNA/target duplexes. RNA *10*, 1507–1517.
24. Itoh, K., Chiba, T., Takahashi, S., Ishii, T., Igarashi, K., Katoh, Y., Oyake, T., Hayashi, N., Satoh, K., Hatayama, I., et al. (1997). An Nrf2/small Maf heterodimer mediates the induction of phase II detoxifying enzyme genes through antioxidant response elements. Biochem. Biophys. Res. Commun. *236*, 313–322.
25. Hirotsu, Y., Katsuoka, F., Funayama, R., Nagashima, T., Nishida, Y., Nakayama, K., Engel, J.D., and Yamamoto, M. (2012). Nrf2-MafG heterodimers contribute globally to antioxidant and metabolic networks. Nucleic Acids Res. *40*, 10228–10239.
26. Talchai, C., Xuan, S., Lin, H.V., Sussel, L., and Accili, D. (2012). Pancreatic β cell dedifferentiation as a mechanism of diabetic β cell failure. Cell *150*, 1223–1234.
27. Donath, M.Y., Ehses, J.A., Maedler, K., Schumann, D.M., Ellingsgaard, H., Eppler, E., and Reinecke, M. (2005). Mechanisms of beta-cell death in type 2 diabetes. Diabetes *54* (*Suppl 2*), S108–S113.

28. Gerber, P.A., and Rutter, G.A. (2017). The Role of Oxidative Stress and Hypoxia in Pancreatic Beta-Cell Dysfunction in Diabetes Mellitus. Antioxid. Redox Signal. *26*, 501–518.

29. Li, N., Frigerio, F., and Maechler, P. (2008). The sensitivity of pancreatic beta-cells to mitochondrial injuries triggered by lipotoxicity and oxidative stress. Biochem. Soc. Trans. *36*, 930–934.

30. Ohlsson, H., Karlsson, K., and Edlund, T. (1993). IPF1, a homeodomain-containing transactivator of the insulin gene. EMBO J. *12*, 4251–4259.

31. Kaneto, H., Xu, G., Fujii, N., Kim, S., Bonner-Weir, S., and Weir, G.C. (2002). Involvement of c-Jun N-terminal kinase in oxidative stress-mediated suppression of insulin gene expression. J. Biol. Chem. *277*, 30010–30018.

32. Keane, K.N., Cruzat, V.F., Carlessi, R., de Bittencourt, P.I., Jr., and Newsholme, P. (2015). Molecular Events Linking Oxidative Stress and Inflammation to Insulin Resistance and β-Cell Dysfunction. Oxid. Med. Cell. Longev. *2015*, 181643.

33. Newsholme, P., Rebelato, E., Abdulkader, F., Krause, M., Carpinelli, A., and Curi, R. (2012). Reactive oxygen and nitrogen species generation, antioxidant defenses, and β-cell function: a critical role for amino acids. J. Endocrinol. *214*, 11–20.

34. Osmai, M., Osmai, Y., Bang-Berthelsen, C.H., Pallesen, E.M., Vestergaard, A.L., Novotny, G.W., Pociot, F., and Mandrup-Poulsen, T. (2016). MicroRNAs as regulators of beta-cell function and dysfunction. Diabetes Metab. Res. Rev. *32*, 334–349.

35. Nesca, V., Guay, C., Jacovetti, C., Menoud, V., Peyot, M.L., Laybutt, D.R., Prentki, M., and Regazzi, R. (2013). Identification of particular groups of microRNAs that positively or negatively impact on beta cell function in obese models of type 2 diabetes. Diabetologia *56*, 2203–2212.

36. Roggli, E., Britan, A., Gattesco, S., Lin-Marq, N., Abderrahmani, A., Meda, P., and Regazzi, R. (2010). Involvement of microRNAs in the cytotoxic effects exerted by proinflammatory cytokines on pancreatic beta-cells. Diabetes *59*, 978–986.

37. Ramachandran, D., Roy, U., Garg, S., Ghosh, S., Pathak, S., and Kolthur-Seetharam, U. (2011). Sirt1 and mir-9 expression is regulated during glucose-stimulated insulin secretion in pancreatic β-islets. FEBS J. *278*, 1167–1174.

38. Du, H., Zhao, Y., Yin, Z., Wang, D.W., and Chen, C. (2021). The role of miR-320 in glucose and lipid metabolism disorder-associated diseases. Int. J. Biol. Sci. *17*, 402–416.

39. Li, H., Fan, J., Zhao, Y., Zhang, X., Dai, B., Zhan, J., Yin, Z., Nie, X., Fu, X.D., Chen, C., and Wang, D.W. (2019). Nuclear miR-320 Mediates Diabetes-Induced Cardiac Dysfunction by Activating Transcription of Fatty Acid Metabolic Genes to Cause Lipotoxicity in the Heart. Circ. Res. *125*, 1106–1120.

40. Yin, Z., Zhao, Y., Du, H., Nie, X., Li, H., Fan, J., He, M., Dai, B., Zhang, X., Yuan, S., et al. (2020). A Key GWAS-Identified Genetic Variant Contributes to Hyperlipidemia by Upregulating miR-320a. iScience *23*, 101788.

41. Laws, S.M., Gaskin, S., Woodfield, A., Srikanth, V., Bruce, D., Fraser, P.E., Porter, T., Newsholme, P., Wijesekara, N., Burnham, S., et al. (2017). Insulin resistance is associated with reductions in specific cognitive domains and increases in CSF tau in cognitively normal adults. Sci. Rep. *7*, 9766.

42. Cao, Z., and Wang, X. (2014). The endocrine role between β cells and intra-islet endothelial cells. Endocr. J. *61*, 647–654.

43. Konstantinova, I., and Lammert, E. (2004). Microvascular development: learning from pancreatic islets. BioEssays *26*, 1069–1075.

44. Ranjan, A.K., Joglekar, M.V., and Hardikar, A.A. (2009). Endothelial cells in pancreatic islet development and function. Islets *1*, 2–9.

45. Brissova, M., Shostak, A., Shiota, M., Wiebe, P.O., Poffenberger, G., Kantz, J., Chen, Z., Carr, C., Jerome, W.G., Chen, J., et al. (2006). Pancreatic islet production of vascular endothelial growth factor–a is essential for islet vascularization, revascularization, and function. Diabetes *55*, 2974–2985.

46. Brindle, N.P., Saharinen, P., and Alitalo, K. (2006). Signaling and functions of angiopoietin-1 in vascular protection. Circ. Res. *98*, 1014–1023.

47. Li, H., Zhang, X., Wang, F., Zhou, L., Yin, Z., Fan, J., Nie, X., Wang, P., Fu, X.D., Chen, C., and Wang, D.W. (2016). MicroRNA-21 lowers blood pressure in spontaneous hypertensive rats by upregulating mitochondrial translation. Circulation *134*, 734–751.

48. Bijkerk, R., Duijs, J.M., Khairoun, M., Ter Horst, C.J., van der Pol, P., Mallat, M.J., Rotmans, J.I., de Vries, A.P., de Koning, E.J., de Fijter, J.W., et al. (2015). Circulating microRNAs associate with diabetic nephropathy and systemic microvascular damage and normalize after simultaneous pancreas-kidney transplantation. Am. J. Transplant. *15*, 1081–1090.

49. Chen, Y.Q., Wang, X.X., Yao, X.M., Zhang, D.L., Yang, X.F., Tian, S.F., and Wang, N.S. (2012). Abated microRNA-195 expression protected mesangial cells from apoptosis in early diabetic renal injury in mice. J. Nephrol. *25*, 566–576.

50. Wang, X.H., Qian, R.Z., Zhang, W., Chen, S.F., Jin, H.M., and Hu, R.M. (2009). MicroRNA-320 expression in myocardial microvascular endothelial cells and its relationship with insulin-like growth factor-1 in type 2 diabetic rats. Clin. Exp. Pharmacol. Physiol. *36*, 181–188.

51. Funkat, A., Massa, C.M., Jovanovska, V., Proietto, J., and Andrikopoulos, S. (2004). Metabolic adaptations of three inbred strains of mice (C57BL/6, DBA/2, and 129T2) in response to a high-fat diet. J. Nutr. *134*, 3264–3269.

52. Hou, T., Zhang, R., Jian, C., Ding, W., Wang, Y., Ling, S., Ma, Q., Hu, X., Cheng, H., and Wang, X. (2019). NDUFAB1 confers cardio-protection by enhancing mitochondrial bioenergetics through coordination of respiratory complex and supercomplex assembly. Cell Res. *29*, 754–766.

53. Brun, T., Assimacopoulos-Jeannet, F., Corkey, B.E., and Prentki, M. (1997). Long-chain fatty acids inhibit acetyl-CoA carboxylase gene expression in the pancreatic beta-cell line INS-1. Diabetes *46*, 393–400.

54. Chen, C., Yang, S., Li, H., Yin, Z., Fan, J., Zhao, Y., Gong, W., Yan, M., and Wang, D.W. (2017). Mir30c Is Involved in Diabetic Cardiomyopathy through Regulation of Cardiac Autophagy via BECN1. Mol. Ther. Nucleic Acids *7*, 127–139.

55. Huang, J., Meng, Y., Liu, Y., Chen, Y., Yang, H., Chen, D., Shi, J., and Guo, Y. (2016). MicroRNA-320a Regulates the Osteogenic Differentiation of Human Bone Marrow-Derived Mesenchymal Stem Cells by Targeting HOXA10. Cell. Physiol. Biochem. *38*, 40–48.

56. Devereux, R.B., Roman, M.J., Paranicas, M., O'Grady, M.J., Lee, E.T., Welty, T.K., Fabsitz, R.R., Robbins, D., Rhoades, E.R., and Howard, B.V. (2000). Impact of diabetes on cardiac structure and function: the strong heart study. Circulation *101*, 2271–2276.

57. Walters, S., Webster, K.E., Sutherland, A., Gardam, S., Groom, J., Liuwantara, D., Mariño, E., Thaxton, J., Weinberg, A., Mackay, F., et al. (2009). Increased CD4+Foxp3+ T cells in BAFF-transgenic mice suppress T cell effector responses. J. Immunol. *182*, 793–801.

58. Koulajian, K., Ivovic, A., Ye, K., Desai, T., Shah, A., Fantus, I.G., Ran, Q., and Giacca, A. (2013). Overexpression of glutathione peroxidase 4 prevents β-cell dysfunction induced by prolonged elevation of lipids in vivo. Am. J. Physiol. Endocrinol. Metab. *305*, E254–E262.

59. Xie, J., Ameres, S.L., Friedline, R., Hung, J.H., Zhang, Y., Xie, Q., Zhong, L., Su, Q., He, R., Li, M., et al. (2012). Long-term, efficient inhibition of microRNA function in mice using rAAV vectors. Nat. Methods *9*, 403–409.

60. Loh, K., Shi, Y.C., Walters, S., Bensellam, M., Lee, K., Dezaki, K., Nakata, M., Ip, C.K., Chan, J.Y., Gurzov, E.N., et al. (2017). Inhibition of Y1 receptor signaling improves islet transplant outcome. Nat. Commun. *8*, 490.